

## Degradation of organometallic perovskite solar cells induced by trap states

Dandan Song,<sup>1</sup> Jun Ji,<sup>1</sup> Yaoyao Li,<sup>1</sup> Guanying Li,<sup>1</sup> Meicheng Li,<sup>1,2,a)</sup> Tianyue Wang,<sup>1</sup> Dong Wei,<sup>1</sup> Peng Cui,<sup>1</sup> Yue He,<sup>1</sup> and Joseph Michel Mbengue<sup>1</sup>

<sup>1</sup>State Key Laboratory of Alternate Electrical Power System with Renewable Energy Sources, School of Renewable Energy, North China Electric Power University, Beijing 102206, China

<sup>2</sup>Chongqing Materials Research Institute, Chongqing 400707, China

(Received 25 November 2015; accepted 17 February 2016; published online 2 March 2016)

The degradation of organometallic perovskite solar cells (PSCs) is the key bottleneck hampering their development, which is typically ascribed to the decomposition of perovskite ( $\text{CH}_3\text{NH}_3\text{PbI}_3$ ). In this work, the degradation of PSCs is observed to be significant, with the decrease in efficiency from 18.2% to 11.5% in ambient air for 7 days. However, no obvious decomposition or structural evolution of the perovskite was observed, except the notable degradation phenomenon of the device. The degradation of PSCs derives from deteriorated photocurrent and fill factor, which are proven to be induced by increased trap states for enlarged carrier recombination in degraded PSCs. The increased trap states in PSCs over storage time are probably induced by the increased defects at the surface of perovskite. The trap states induced degradation provides a physical insight into the degradation mechanisms of PSCs. Moreover, as the investigations were performed on real PSCs instead of individual perovskite films, the findings here present one of their actual degradation mechanisms. © 2016 AIP Publishing LLC. [<http://dx.doi.org/10.1063/1.4943019>]

Organometallic perovskite materials ( $\text{CH}_3\text{NH}_3\text{PbX}_3$ ,  $\text{X} = \text{Cl}, \text{Br}, \text{I}$ ) have shown great promise for application as active materials in solar cells in the past several years.<sup>1-4</sup> Owing to the enormous efforts on the structural and material optimization, the power conversion efficiency (PCE) of lead halide perovskite based thin film solar cells (PSCs) has increased to more than 20%,<sup>5,6</sup> which approaches to that of mono-crystalline silicon solar cells. Aside from the power conversion efficiency, the device stability is another key issue in determining the application of PSCs in the industry.<sup>7</sup> The degradation of the PSCs should be urgently addressed to achieve good reproducibility and long lifetime for highly efficient PSCs. The material stability of perovskite and the related degradation mechanism are typically used to explain the stability of PSCs.<sup>8-10</sup> The origin of the material stability of perovskite is ascribed to the decomposition of perovskite under different atmospheres and conditions.<sup>8,10,11</sup> Moisture is found to be a critical factor in governing the decomposition of perovskite ( $\text{CH}_3\text{NH}_3\text{PbI}_3$ ).<sup>9,10,12</sup> The decomposition of perovskite leads to the formation of  $\text{PbI}_2$ <sup>9,12,13</sup> or hydrate product<sup>9,13</sup> according to different studies, causing the decrease in the absorption across the visible region and a distinct change in crystal structure of the material.

However, concerns need to be paid on the explanations for the stability of PSCs on the basis of material stability. The findings focusing on the degradation mechanisms of perovskite are typically obtained from individual perovskite films rather than from complete solar cells.<sup>8,9</sup> Though the roles of these degradation mechanisms on the electronic processes (for example, carrier recombination and carrier transport processes) in the PSCs can be deduced to some extent, exploring direct evidences needs the packing of the films into devices. Meanwhile, the circumstance of the perovskite in PSCs is also

different from that of the individual perovskite film, as the presence of hole transport material (HTM) and metal electrode protect the perovskite film<sup>13,14</sup> from outer circumstances, which are factors that are crucial in determining the degradation of perovskite films. Therefore, the degradation of PSCs is not suitable to be simply explained by the degradation mechanisms of the perovskite, which needs to be carefully explored. Moreover, the degradation of the optoelectronic devices including solar cells correlates with the physical processes and/or interfacial features<sup>9,15,16</sup> in addition to the material stability. However, these factors are not able to be examined by individual films but of great importance and require more explorations.

In this work, the degradation of the PSCs is observed to be significant in ambient condition, which is caused by the increased trap states proved by current-voltage characteristics and open-circuit voltage decay measurements. The decomposition or structure evolution of the perovskite film has not been detected by the x-ray diffraction patterns and the absorption spectra. All of the investigations were performed on PSCs or the perovskite films extracted from PSCs by removal of Au electrode and HTM. Hence, it is concluded that the degradation by trap states is one of the real mechanisms for the degradation of PSCs.

$\text{CH}_3\text{NH}_3\text{PbI}_3$  films were fabricated using a modified sequential deposition process as illustrated in our previous work.<sup>17,18</sup> The solar cells employ the planar architecture of F-doped tin oxide (FTO)/compact  $\text{TiO}_2$ / $\text{CH}_3\text{NH}_3\text{PbI}_3$  (~300 nm)/HTM/Au electrode. The HTM used here is 2, 2', 7, 7'-tetrakis[*N*, *N*-di(4-methoxyphenyl)amino]-9, 9'-spirobifluorene (spiro-MeOTAD) with the standard additives including *tert*-butylpyridine and lithium bis(trifluoromethanesulfonyl)imide. For examining the perovskite film in the PSCs, Au electrode and HTM are occasionally removed. The removal of Au electrode was carried out by tape peeling method with scotch tape,<sup>19</sup> which can remove Au electrode perfectly from the organic

<sup>a)</sup> Author to whom correspondence should be addressed. Electronic mail: [mcli@ncepu.edu.cn](mailto:mcli@ncepu.edu.cn). Tel: +86 10 6177 2951. Fax: +86 10 6177 2951.

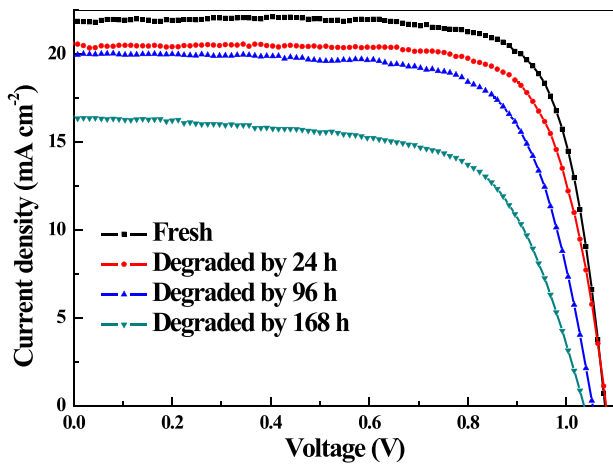


FIG. 1. J-V curves of the PSCs measured with a reverse scan rate of 150 mV/s after different storage times.

HTM due to the weak bonding between metal-organic materials. The removal of HTM layer from the residual PSC stack (FTO/TiO<sub>2</sub>/perovskite/HTM) was achieved by washing the stacks with chlorobenzene for 3 times, because HTM can be quickly dissolved in chlorobenzene whereas perovskite is insoluble. The degradation process of the PSCs was carried out in ambient atmosphere without encapsulation for 168 h (7 days). Photocurrent-voltage (J-V) curves of the PSCs monitored immediately after fabrication (fresh), 24 h, 96 h and 168 h after fabrication are shown in Fig. 1. It can be seen that the fresh PSC shows excellent performance, with a short circuit current ( $J_{SC}$ ) of 21.9 mA cm<sup>-2</sup>, an open circuit voltage ( $V_{OC}$ ) of 1.08 V, and a fill factor (FF) of 76.9%, leading to a PCE of 18.2%. However, the performance of the PSCs degrades consistently with the increase in storage time. As shown in Fig. 1,  $V_{OC}$  shows small degradation from 1.08 V to 1.04 V after stored for 168 h. However,  $J_{SC}$  and FF decrease obviously, leading to the low PCE of 11.0%. Table I gives the average values of photovoltaic parameters from multiple identical PSCs. The average PCE of the PSCs is degraded to approach 50% after stored for 168 h (7 days) in ambient air.

To study the degradation kinetics of the PSCs, the electrical parameters of the solar cells, including the series resistance ( $R_s$ ), the shunt resistance ( $R_{sh}$ ), the reverse saturation current ( $J_0$ ), and the diode ideality factor ( $m$ ), were extracted from J-V curves using Origin software by fitting them with the equation

$$J = J_{SC} - J_0 \left[ \exp \left( \frac{-q(V + AJR_s)}{mk_B T} \right) - 1 \right] - \frac{V + AJR_s}{AR_{sh}},$$

TABLE I. Photovoltaic parameters of the fresh and degraded PSCs. The standard deviation of the PSCs was obtained from 5 identical solar cells.

PSCs	$J_{SC}$ (mA cm <sup>-2</sup> )	$V_{OC}$ (V)	FF (%)	PCE (%)	Max. PCE (%)
Fresh	21.2 ± 0.7	1.06 ± 0.01	73.8 ± 2.3	16.6 ± 0.9	18.2
24 h	19.9 ± 1.3	1.06 ± 0.01	73.6 ± 1.3	15.6 ± 1.3	17.0
96 h	18.6 ± 1.9	1.04 ± 0.02	69.3 ± 2.0	13.5 ± 1.9	15.6
168 h	16.1 ± 1.5	1.01 ± 0.03	53.8 ± 7.4	8.8 ± 2.1	11.5

TABLE II. Fitted electrical parameters of the fresh and degraded PSCs.

Solar cells	$R_s$ (Ω)	$R_{sh}$ (kΩ)	$J_0$ (mA cm <sup>-2</sup> )	$M$	$J_{SC}$ (mA cm <sup>-2</sup> )
Fresh	60.61	1395	2.12E-6	2.60	21.99
24 h	157.59	1138	8.09E-6	2.86	20.54
96 h	354.27	359	2.31E-5	3.01	20.07
168 h	653.70	117	5.32E-5	3.22	16.58

where  $A$  and  $m$  represent for the device area and the diode ideality factor, respectively. The calculated values are listed in Table II. It is clear that all of the electrical parameters are worse in degraded PSCs.  $R_s$  increases with the degradation time of the PSCs, which reflects increased bulk resistance, leading to lowered  $J_{SC}$  and FF.  $R_{sh}$  is large enough for both of degraded and fresh PSCs, causing minor change of  $V_{OC}$ . These results are consistent with the degradation in the photovoltaic performance of the PSCs.  $J_0$  correlates with the carrier recombination in p- and n-region, so higher  $J_0$  from degraded PSCs corresponds to higher carrier recombination in these regions than that from the fresh PSC.

The calculated ideality factor ( $m$ ) of the PSCs is larger than 2 (Table II), which is higher than the typical values for other solar cells (1–2) or phenyl-C61-butyric acid methyl ester (PCBM)-based PSCs (~1.8).<sup>20</sup> Different from other solar cells, PSCs are reported to yield ion migration under electric field, which probably cause the PSCs deviating from the ideal diodes (a high ideality factor). In PCBM-PSCs, the ions can be tied up through the formation of a PCBM-halide radical,<sup>21</sup> leading to a much rational ideality factor.<sup>20</sup> A high ideality factor indicates the recombination current in the space charge region is the main contribution to the dark current. The high ideality factor with increasing degradation time indicates enhanced carrier recombination in the degraded PSCs. Hence, the dark current of the fresh and degraded PSCs is characterized and shown in Fig. 2(a). The dark current at the low voltage scale (mainly determined by the recombination current) is higher in the degraded PSC, whereas the current after the threshold voltage (mainly determined by the diffusion current) is lower. As the recombination of the PSCs is evidenced to be governed by the trap states,<sup>20</sup> the higher recombination current in the degraded PSC indicates more severe recombination and more trap states in its space charge region. The lower current after the threshold voltage in the degraded PSC corresponds to its high  $R_s$ . Hence, it can be deduced that the number of the traps states is enlarged in the degraded PSCs, which leads to the increased carrier losses and the deteriorated performance of the PSCs.

Open circuit voltage decay (OCVD) characters also reveal the increased carrier recombination and trap states in the degraded PSCs. As shown in Fig. 2(b), the decay curves of  $V_{OC}$  at different irradiation intensities or measured at different storage times are all composed of a slow decay, which is similar to the previous report.<sup>22</sup> The slow decay component of  $V_{OC}$ , which shows a power law decay and represents for the depolarization of the perovskite,<sup>22</sup> is accelerated after the degradation. This implies the change of the perovskite. Meanwhile, at the initial stage (immediately after the irradiation off) of the  $V_{OC}$  decay curve, the decrease in  $V_{OC}$  is obviously faster in the degraded PSC, implying the faster recombination of the photogenerated carriers induced by the

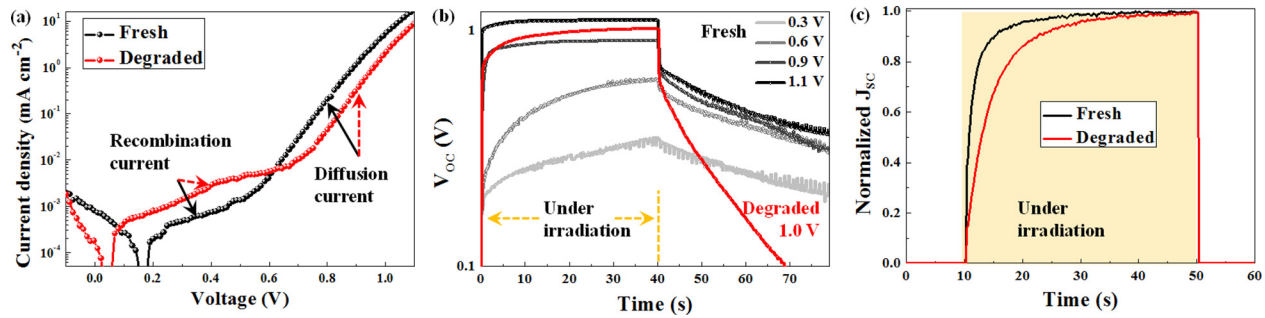


FIG. 2. (a) Dark J-V curves, (b)  $V_{OC}$  decay, and (c) transient  $J_{SC}$  (normalized at maxima) of the fresh and degraded PSCs. The  $V_{OC}$  decay curves were measured at different irradiation intensities to achieve different voltages. The fresh and the degraded PSCs were measured at different storage time (i.e., immediately after fabrication and storage for 7 days, respectively).

enlarged number of the trap states. In our previous work, we show that the fast decay in OCVD curves corresponds to the presence of more trap states and the poor performance of PSCs,<sup>17,18</sup> which are consistent with the case of the degraded PSCs. Moreover, the increased trap states also lead to the slow response of the photocurrent. As shown in Fig. 2(c),  $J_{SC}$  of the degraded PSC increases more slowly after the light on than that of the fresh PSC, further proving the increased trap states during the degradation of PSCs.

Therefore, the increased trap states contribute to the degraded performance of the PSCs. The material origin of the formation of the trap states is investigated and discussed. It may be speculated that the HTM is the material origin for the trap states, which is degraded after storage.<sup>23–25</sup> To testify the speculation, the PSCs based on the degraded PSCs, by renewing the HTM and the Au electrode through removing them from the degraded PSCs and depositing new films, were fabricated. The device performance is recovered by a bit through refreshing HTM (data are not shown here in the interest of saving space), indicating that the trap states are not mainly formed in HTM; otherwise, the device performance will be greatly recovered. Hence, the trap states induced degradation is directly correlated with the perovskite.

The trap states in perovskite are reported to mainly distribute at the surface (including the film surface and the grain boundaries) of the perovskite,<sup>26</sup> so the increased trap states probably correlate with the enlarged perovskite surface (small grains). Hence, the morphology features of the fresh and degraded perovskite films are characterized with scanning electron microscope (SEM), as shown in Fig. 3. The fresh perovskite film shows the typical polycrystalline morphology, with grain size from tens to several hundreds of

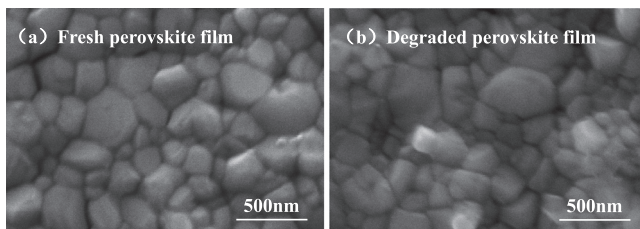


FIG. 3. SEM images of the (a) fresh and (b) degraded perovskite films. The perovskite films were obtained by removing Au electrode and HTM from the PSCs.

nanometers. The degraded perovskite film, obtained from the degraded PSCs by removing Au electrode and HTM, shows similar morphology and grain size, excluding the effect of the morphology evolution on the degradation of the PSCs.

The formation of the trap states in PSCs during degradation is probably due to the formation of  $PbI_2$  or other products, which act as scattering or trap centers in perovskite. Hence, the XRD patterns of fresh and degraded PSCs were measured by removal of Au electrode, which enables the characterization of the actually degraded perovskite films in PSCs. As shown in Fig. 4(a), both of the XRD patterns from fresh and degraded PSCs can be indexed to the diffraction

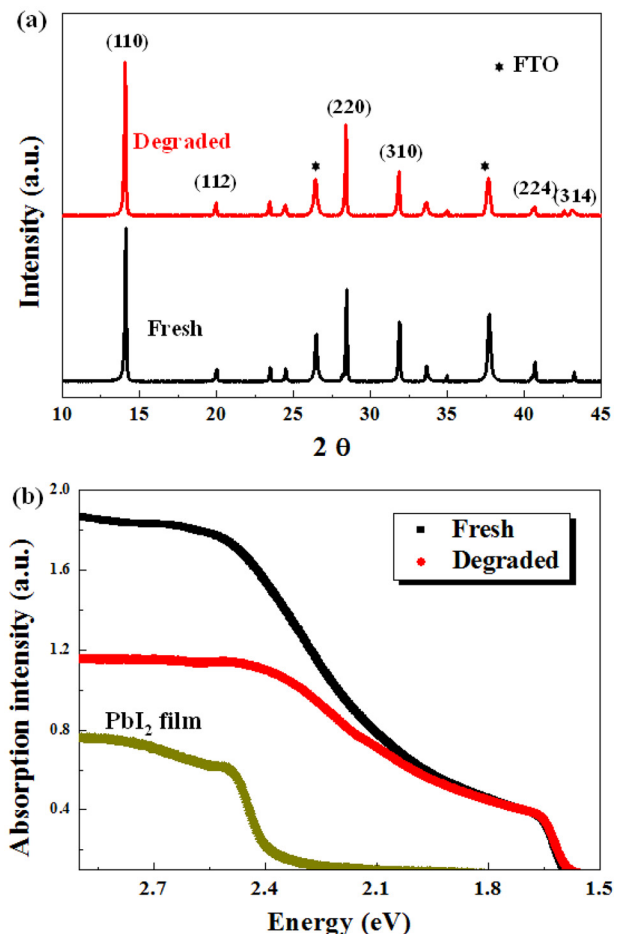


FIG. 4. (a) XRD patterns and (b) absorption spectra of the fresh and degraded PSCs with removal of Au electrode.

peaks of perovskite. The average grain size estimated from the XRD patterns with Scherrer formula is around 70 nm for both the fresh and degraded perovskite films, which is consistent with the SEM measurement. No diffraction peaks from  $\text{PbI}_2$ , typically with an intense peak located at  $12.5^\circ$ , can be observed. Meanwhile, no diffraction peaks from intermediates including perovskite hydrate (with an intense diffraction peak locating at  $10.46^\circ$  (Ref. 9)) are observed. However, the relative peak intensity of (310) plane to that of (110) plane of the perovskite is decreased after degradation. From the XRD spectra in our previous work,<sup>18</sup> it is also observed that the relative peak intensity of (310) plane to that of (110) plane of the perovskite varies with the annealing parameters of the perovskite. In general, a low intensity of (310) plane corresponds to the perovskite films annealed at high temperature or for a long time, the conditions in which perovskite tends to or is decomposed. Hence, it can be speculated that the change in the relative intensity of the diffraction peaks correlates with the change of the perovskite structure, and the (310) plane tends to change more gravely with the annealing parameters. Here, with increasing storage time, the lower intensity of the (310) plane also indicates that a more severe change occurs at this plane, pointing to the fact that the crystal structure of the perovskite starts to deform with the increase in the degradation time. The deformation of the perovskite sites causes the formation of fragments instead of crystalline compounds in the perovskite, because no diffraction peaks from other compounds have been observed in the degraded perovskite. In addition, considering the fact that the morphology of the perovskite changes little after the degradation, hence, only a part of perovskite sites at the surface (film surface and grain boundaries) are possibly changed during degradation. The chemical origin for the change of the perovskite is probably the migration of the ions, which cause the change in the crystal structure of the perovskite and simultaneously induce defects, including the vacancies or interstitials at the surface of the perovskite. The interaction between perovskite and the additives in HTM or the moisture may also promote the formation of the trap states at the surface of the perovskite. Further investigations need to be carried out.

The optical absorption spectra of the PSCs (by removal of Au electrode) were also characterized. As shown in Fig. 4(b), the absorption spectra of the fresh and degraded PSCs show similar shape, exhibiting the typical absorption feature of the perovskite. The characteristic absorption of  $\text{PbI}_2$  (as shown in Fig. 4(b) from pure  $\text{PbI}_2$  film) locates at the region higher than 2.4 eV, in which scale the absorption of the degraded PSC is much lower. Therefore, the degradation of the PSCs is not caused by the decomposition of the perovskite to  $\text{PbI}_2$ , which otherwise will compensate the absorption at high energy scale in the degraded PSC. The lower absorption intensity of the degraded PSC, in comparison to that of the fresh one, indicates that a part of the perovskite sites are changed by degradation, which is in accordance with the XRD results. As the absorption spectra changes little after degradation, it can be speculated that the formed fragments yield low absorption coefficient, which only cause the reduction in the absorption intensity without modifying the shape of the absorption spectra.

Therefore, the increased number of the trap states over degradation time is not caused by either morphology evolution or the decomposition of perovskite to  $\text{PbI}_2$  or perovskite hydrate. Instead, it is due to the formation of the fragments deriving from the change in the crystal structure of partial perovskite sites at the perovskite surface. As the energy level of the perovskite is created by the unoccupied Pb  $p$  orbital and occupied I  $p$  orbital in the perovskite structure,<sup>27</sup> the change in the partial perovskite sites from their ideal crystal structure will induce the formation of additional energy levels at the perovskite surface. These additional energy levels can act as trapping centers for carriers; hence, the trap states are increased in the degraded PSCs and cause the deterioration in device performance.

In conclusion, the degradation of the perovskite solar cells is proved to be assisted by increased trap states, which cause enlarged carrier recombination and lowered device photovoltaic performance. Moreover, no decomposition or morphology evolution of the perovskite film was observed, demonstrating its good component and structure stability in the perovskite solar cells. The trap states of the perovskite solar cells need to be further explored to achieve highly efficient and stable perovskite solar cells. This work provides physical insights in the degradation mechanism of the perovskite solar cells, which also highlights the importance of exploring methods to reduce the trap states for highly efficient and stable perovskite solar cells.

This work was partially supported by National High-tech R&D Program of China (863 Program, No. 2015AA034601), National Natural Science Foundation of China (Grant Nos. 91333122, 61204064, 51202067, 51372082, 51402106, and 11504107), Ph.D. Programs Foundation of Ministry of Education of China (Grant Nos. 20120036120006 and 20130036110012), Par-Eu Scholars Program, and the Fundamental Research Funds for the Central Universities.

<sup>1</sup>A. Kojima, K. Teshima, Y. Shirai, and T. Miyasaka, *J. Am. Chem. Soc.* **131**, 6050 (2009).

<sup>2</sup>J. H. Im, C. R. Lee, J. W. Lee, S. W. Park, and N. G. Park, *Nanoscale* **3**, 4088 (2011).

<sup>3</sup>Z. Zhang, X. Zhao, T. Wang, Y. Zhao, C. Shen, and M. Trevor, *Energy Environ. Focus* **3**, 354 (2014).

<sup>4</sup>H. Zhou, Q. Chen, G. Li, S. Luo, T. B. Song, H. S. Duan, Z. Hong, J. You, Y. Liu, and Y. Yang, *Science* **345**, 542 (2014).

<sup>5</sup>W. S. Yang, J. H. Noh, N. J. Jeon, Y. C. Kim, S. Ryu, J. Seo, and S. I. Seok, *Science* **348**, 1234 (2015).

<sup>6</sup>M. A. Green, E. Keith, H. Yoshihiro, W. Wilhelm, and E. D. Dunlop, *Prog. Photovoltaics: Res. Appl.* **23**, 805 (2015).

<sup>7</sup>M. A. Green and T. Bein, *Nat. Mater.* **14**, 559 (2015).

<sup>8</sup>I. C. Smith, E. T. Hoke, D. Solis-Ibarra, M. D. McGehee, and H. I. Karunadasa, *Angew. Chem. Int. Ed.* **53**, 11232 (2014).

<sup>9</sup>J. A. Christians, P. A. Miranda Herrera, and P. V. Kamat, *J. Am. Chem. Soc.* **137**, 1530 (2015).

<sup>10</sup>G. Niu, W. Li, F. Meng, L. Wang, H. Dong, and Y. Qiu, *J. Mater. Chem. A* **2**, 705 (2014).

<sup>11</sup>I. Deretzis, A. Alberti, G. Pellegrino, E. Smecca, F. Giannazzo, N. Sakai, T. Miyasaka, and A. L. Magna, *Appl. Phys. Lett.* **106**, 131904 (2015).

<sup>12</sup>R. K. Misra, S. Aharon, B. Li, D. Mogilyansky, I. Visoly-Fisher, L. Etgar, and E. A. Katz, *J. Phys. Chem. Lett.* **6**, 326 (2015).

<sup>13</sup>J. Yang, B. D. Siempelkamp, D. Liu, and T. L. Kelly, *ACS Nano* **9**, 1955 (2015).

<sup>14</sup>J. Xiao, J. Shi, H. Liu, Y. Xu, S. Lv, Y. Luo, D. Li, Q. Meng, and Y. Li, *Adv. Energy Mater.* **5**, 1401943 (2015).

- <sup>15</sup>Q. Wang, B. Sun, and H. Aziz, *Adv. Funct. Mater.* **24**, 2975 (2014).
- <sup>16</sup>O. A. Jaramillo-Quintero, R. S. Sanchez, M. Rincon, and I. Mora-Sero, *J. Phys. Chem. Lett.* **6**, 1883 (2015).
- <sup>17</sup>P. Cui, P. Fu, D. Wei, M. Li, D. Song, X. Yue, Y. Li, Z. Zhang, Y. Li, and J. M. Mbengue, *RSC Adv.* **5**, 75622 (2015).
- <sup>18</sup>D. Song, P. Cui, T. Wang, D. Wei, M. Li, F. Cao, X. Yue, P. Fu, Y. Li, Y. He, B. Jiang, and M. Trevor, *J. Phys. Chem. C* **119**(40), 22812 (2015).
- <sup>19</sup>Q. Wang, Y. Luo, and H. Aziz, *Appl. Phys. Lett.* **97**, 063309 (2010).
- <sup>20</sup>G. J. A. Wetzelaer, M. Scheepers, A. M. Sempere, C. Momblona, J. Ávila, and H. J. Bolink, *Adv. Mater.* **27**, 1837 (2015).
- <sup>21</sup>J. Xu, A. Buin, A. H. Ip, W. Li, O. Voznyy, R. Comin, M. Yuan, S. Jeon, Z. Ning, J. J. McDowell *et al.*, *Nat. Commun.* **6**, 7081 (2015).
- <sup>22</sup>L. Bertoluzzi, R. S. Sanchez, L. Liu, J.-W. Lee, E. Mas-Marza, H. Han, N.-G. Park, I. Mora-Sero, and J. Bisquert, *Energy Environ. Sci.* **8**, 910 (2015).
- <sup>23</sup>N. H. Severin, L. Tomas, E. E. Giles, D. S. Samuel, J. N. Robin, and J. S. Henry, *Nano Lett.* **14**, 5561 (2014).
- <sup>24</sup>M. T. Tsai, F. Y. Chang, Y. C. Yao, J. Mei, and Y. J. Lee, *Sol. Energy Mater. Sol. Cells* **136**, 193 (2015).
- <sup>25</sup>F. Matteocci, S. Razza, F. D. Giacomo, S. Casaluci, G. Mincuzzi, T. M. Brown, A. D'Epifanio, S. Licoccia, and A. D. Carlo, *Phys. Chem. Chem. Phys.* **16**, 3918 (2014).
- <sup>26</sup>X. Wu, M. T. Trinh, D. Niesner, H. Zhu, Z. Norman, J. S. Owen, O. Yaffe, B. J. Kudisch, and X.-Y. Zhu, *J. Am. Chem. Soc.* **137**, 2089 (2015).
- <sup>27</sup>W. Yin, T. Shi, and Y. Yan, *Appl. Phys. Lett.* **104**, 063903 (2014).